X-RAY OBSERVATIONS OF THE PECULIAR CEPHEID V473 LYR IDENTIFY A LOW–MASS COMPANION [1],

Nancy Remage Evans,[2] Ignazio Pillitteri,[3] Laszlo Molnar,[4] Laszlo Szabados,[4] Emese Plachy,[4] Robert Szabo,[4] Scott Engle,[5] Edward Guinan,[5] Scott Wolk,[2] H. Moritz Günther,[6] Hilding Neilson,[7] Massimo Marengo,[8] Lynn D. Matthews,[9] Sofia Moschou,[2] Jeremy J. Drake,[2] Vinay Kashyap,[2] Pierre Kervella,[10] Tamas Tordai,[11] Peter Somogyi,[12] and Gilbert Burki[13]

[1] Based on observations obtained with *XMM-Newton*, an ESA science mission with instruments and contributions directly funded by ESA Member States and the USA (NASA)

[2] Smithsonian Astrophysical Observatory, MS 4, 60 Garden St., Cambridge, MA 02138; nevans@cfa.harvard.edu

[3] INAF-Osservatorio di Palermo, Piazza del Parlamento 1, 90134 Palermo, Italy

[4] Konkoly Observatory, and MTA CSFK Lendület Near-Field Cosmology Research Group, Konkoly Thege Miklos ut 15-17, H-1121 Budapest, Hungary

[5] Department of Astronomy and Astrophysics, Villanova University, 800 Lancaster Ave., Villanova, PA, 19085, USA

[6] Massachusetts Institute of Technology, Kavli Institute for Astrophysics and Space Research, 77 Massachusetts Ave, NE83-569, Cambridge MA 02139, USA

[7] Department of Astronomy and Astrophysics, University of Toronto, 50 St. George Street, Toronto, ON, Canada M5S3H4

[8] Department of Physics and Astronomy, Iowa State University, Ames, IA, 50011, USA

[9] Massachusetts Institute of Technology, Haystack Observatory, 99 Millstone Rd., Westford, MA 01886, USA

[10] LESIA, Observatoire de Paris, Université PSL, CNRS, Sorbonne Université, Univ. Paris Diderot, Sorbonne Paris Cité, 5 place Jules Janssen, 92195 Meudon, France

[11] Polaris Observatory, Hungarian Astronomical Association, Laborc utca 2/c, 1037 Budapest, Hungary

[12] Zrinyi u. 23., 2890, Tata, Hungary

[13] Observatoire de Genve, 51 chemin des Maillettes, 1290 Sauverny, Switzerland

ABSTRACT

V473 Lyr is a classical Cepheid which is unique in having substantial amplitude variations with a period of approximately 3.3 years, thought to be similar to the Blazhko variations in RR Lyrae stars. We obtained an *XMM-Newton* observation of this star to followup a previous detection in X-rays. Rather than the X-ray burst and rapid decline near maximum radius seen in δ Cephei itself, the X-ray flux in V473 Lyr remained constant for a third of the pulsation cycle covered by the observation. Thus the X-rays are most probably not produced by the changes around the pulsation cycle. The X-ray spectrum is soft (kT = 0.6 keV), with X-ray properties which are consistent with a young low mass companion. Previously there was no evidence of a companion in radial velocities or in *Gaia* and *Hipparcos* proper motions. While this rules out companions which are very close or very distant, a binary companion at a separation between 30 and 300 AU is possible. This is an example of an X-ray observation revealing evidence of a low mass companion, which is important in completing the mass ratio statistics of binary Cepheids. Furthermore, the detection of a young X-ray bright companion is a further indication that the Cepheid (primary) is a Population I star, even though its pulsation behavior differs from other classical Cepheids.

Keywords: stars: Cepheids: binaries; stars:massive; stars: variable; X-rays

1. INTRODUCTION

Pop I classical Cepheids are radial pulsators that have very regular pulsation cycles. Complicated photometric variations, however, are found in a small group which are excited in two modes. Long series of precise photometry from satellites such as *Kepler*, *MOST*, and *CoRoT* have begun to alert us to additional excited frequencies, particularly in overtone pulsators. The notable exception to the regular pulsation is V473 Lyr, which has a variable amplitude of pulsation. The main pulsation period is 1.49^d, with a period of amplitude variation of 1205^d. Existing data are discussed by Molnar and Szabados (2014; MS below). This amplitude variation appears to be similar to the Blazhko

effect seen in many RR Lyr stars. As discussed there, V473 Lyr is thought to be pulsating in the second overtone. A number of explanations have been put forward for the amplitude variation, but the most likely is the resonance between two pulsation modes, which is discussed by MS. They identified an additional modulation cycle of 5300^d. A sequence of 27 days of observations with the *MOST* satellite (Molnar, et al. 2017) shows period doubling (the alternation of the amplitudes of successive cycles). This is seen in RV Tau and RR Lyr Pop II pulsators, but this is the first case in a Pop I classical Cepheid.

X-ray observations of classical Cepheids have a peculiar pattern (Engle, et al. 2017). The pulsation cycle results in disturbances in the photosphere and chromosphere following minimum radius as the pulsation wave passes through. X-ray flux of δ Cep is relatively modest and constant at this phase. Just after maximum radius, however, the X-ray flux increases sharply by a factor of approximately four. At this phase, photospheric and chromospheric spectra are quiescent, indistinguishable from those of nonvariable supergiants. This pattern is seen in two cycles of δ Cep and in β Dor.

V473 Lyr was observed by the *XMM* satellite in a program to observe 14 Cepheids (Evans, et al. 2016a), which was developed from observations using the *Hubble Space Telescope (HST)* Widefield Camera 3 (WFC3) to identify possible resolved companions (Evans, et al. 2016b). The *XMM* observations were used to distinguish X-ray active low mass stars young enough to be Cepheid companions from old field stars which are much less active. V473 Lyr was found to have an X-ray source at the position of the Cepheid. Table 1 lists the phase of the observation based on complex pulsation behavior discussed in MS. The phase of the X-ray observation was found to be the same as the phase at which δ Cep has a burst of X-rays, namely just after maximum radius (Evans, et al. 2018). This suggests the possibility that the X-ray flux was produced in the same way as for δ Cep. For this reason an additional *XMM* observation was applied for, partly to use the variation in pulsation amplitude as a diagnostic of the effect.

Table 1.　*XMM* Observations of V473 Lyr

Year		JD −2400000	Exp ksec	Phase
2019	Start	58559.762	40.3	0.42
	End	58560.228		0.73
2013	Start	56557.909	6.6	0.47
	End	56558.002		0.53

2. OBSERVATION AND DATA ANALYSIS

2.1. *XMM Observation*

A new observation of V473 Lyr with *XMM* was obtained in 2019 (Table 1). Data analysis was carried out using standard data reduction tasks in SAS software (Scientific Analysis Subsystem) version 17.0 as in Pillitteri, et al. (2013). This involved a reduction starting from the ODFs of the observation, filtering the events according to their grades and screening out bad pixels. Only events between 0.3 and 8.0 keV were used, and the reduction was restricted to good time intervals and low background periods. These were evaluated using the recipe given in the SAS guidelines and based on the light curve of the events above 10 keV.

Again there was a source at the position of the Cepheid. The light variation (PN chip array) and the spectrum are shown in Fig. 1 and Fig. 2. Fig. 1 shows that the flux is essentially constant during the exposure. Fig 2 shows the spectrum fit given for a temperature of kT = 0.6 keV (using a H column density of 3×10^{21} cm^{-2} [appropriate for a low E(B-V) = 0.03 mag] and an abundance of 0.3 Z$_\odot$). The unabsorbed flux is 3.2×10^{-14} erg cm^{-2} s^{-1} in the 0.3 to 8.0 keV band. Using a distance of 553 pc (Evans, et al. 2016b), this is log Lx = 30.07 erg s^{-1}. This distance is based on the Benedict, et al. (2007) Leavitt Law. This is larger than the distance calculated from the data in the *Gaia* DR2 catalog (*Gaia* Collaboration et al. 2018).

We have tested whether variability is detectable in the light curve Fig. 1 using the observed fluctuations in the counts against a constant count rate model. We account for the presence of a constant background rate, and exclude times when the PN background flares. We compute a `cstat` value (Cash statistic; Cash 1979) and corresponding approximate goodness-of-fit measure (Kaastra 2017) for the data compared with the averaged counts in light curves binned from 100 to 1000 s. We have also compared the histogram of counts from a binned counts light curve against the predicted Poisson frequency. The PN data have the most counts, but we have also examined MOS1 and MOS2 both separately and together. The results varied depending on the detector and time bin, but we find marginal evidence for variability at the largest binning at the 10% level.

2.2. *Photometry*

Since the pulsation amplitude of V473 Lyr is variable, photometry was obtained near the time of the *XMM* observation to confirm the phases. Observations were made near Budapest, Hungary, with a 15 cm telescope, and an Orion StarShoot G3 CCD camera, in the V band. During the first night, defocused images were taken with 5 sec integrations to avoid saturation. For the second night the telescope was used with an aperture opening reduced to 4 cm diameter, with 30 sec integration times. HD 180316 (V = 6.891 mag) and HD 337922 (V = 9.171 mag) were used as comparison and check stars. Differential magnitudes were shifted to the average brightness of the star (V = 6.153 mag), and times were converted to HJD. Data are listed in Appendix A (full table in the electronic version). The data were binned (20 points) to decrease the scatter. Since the pulsation at this time is at a low-amplitude phase and the light curve is nearly sinusoidal, we fitted the observations with a simple sine, with the frequency fixed to the average pulsation frequency value ($0.67079 \ \mathrm{d}^{-1}$). This way we were able to confirm the pulsation phase during the observing window for XMM-Newton. As Fig. 3 shows, data collection started slightly before minimum light, and ended about halfway up the ascending branch.

Fig. 4 shows the updated phase variation of V473 Lyr, with the photometry from Fig. 3 included.

2.3. *Velocities: 2019*

Radial velocity data were collected on two nights from Hungary with a 30 cm Newton telescope, and a Shelyak LHires III spectrograph, at R 13000 resolution, on 17th March, 2019, right before the XMM run started, and again on the 24th, for 2.3 and 2.7 hours, respectively. An Ar/Ne calibration lamp and the radial velocity standard star 45 Dra were used for wavelength calibration. Images were processed with ISIS[1], then the spectra were rectified with IRAF[2]. Lines between 6103 and 6223 Å were used to determine the radial velocities with the IRAF cross-correlation task fxcor. Uncertainties for the target and standard star measurements were both estimated to be 0.5 km/s. Velocities are listed in Appendix B (full table in the electronic version).

2.4. *TESS Observations*

V473 Lyr was observed by the TESS space telescope in Sector 14, a few months after the XMM run, from July 18th to August 14, 2019 (Ricker et al., 2014). Observations were made in short cadence mode, with 2 min sampling. We analyzed the light curve released by the Spacecraft Operations Center (SPOC) and created custom-aperture photometry with our *lightkurve* package (Lightkurve Collaboration, 2018 [3]) which is shown in Fig. 5. Since the star is in a low-amplitude phase and TESS observes in a broad red bandpass (between 600-1000 nm), the peak-to-peak pulsation amplitude was very small, only 41 mmag. We detected the main pulsation peak (f), its first harmonic, and one side peak that is connected with the modulation, along with some low-frequency components that are likely caused by blending with nearby stars and other noise sources. We looked for signs of period doubling, and we found a low-amplitude frequency component at 1.5f, but given the presence of low-frequency noise in the frequency spectrum nearby, we cannot claim unambiguous detection. However, this is not necessarily at odds with the earlier results, for two reasons. First, MOST observed the star in shorter wavelengths where Cepheid pulsation amplitudes are higher, making detection easier. Second, the amplitude of period doubling was found to fluctuate rather erratically in RR Lyrae stars: if V473 Lyr behaves similarly, non-detection from a short data set can be expected (Szabo et al. 2010). We also looked for any signs of flaring activity in the residual light curve, but found none with an upper limit of 1 mmag.

---

[1] http://www.astrosurf.com/buil/isis-software.html

[2] http://ui.adsabs.harvard.edu/abs/1986SPIE..627..733T

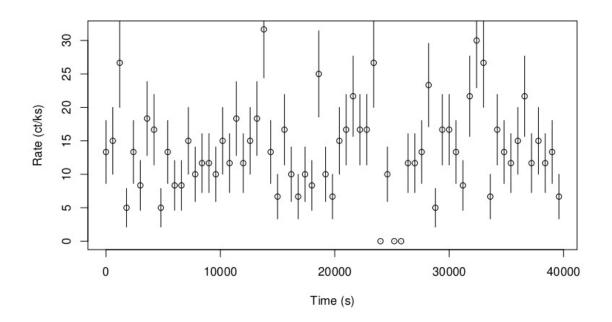[3] http://adsabs.harvard.edu/abs/2018ascl.soft12013L

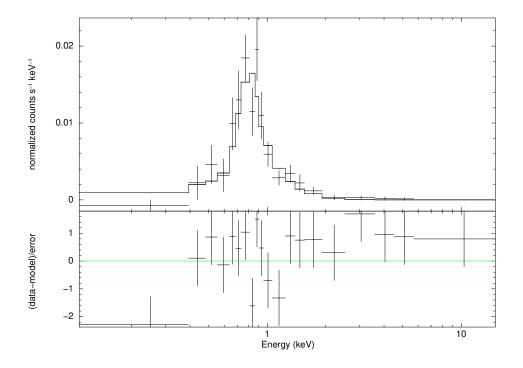**Figure 1**. Count rate during the *XMM* exposure.

Figure 2. Extracted spectrum of V473 Lyr. Top: +'s: data; histogram: data fit. Bottom: residuals.
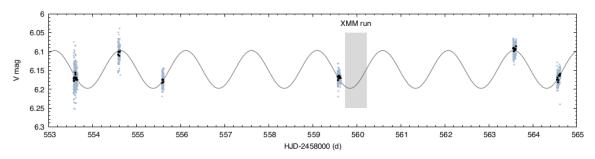
Figure 3. New photometric data and the phases of the *XMM* observation. Blue dots: V magnitude data; black dots: 20 point binned data; solid line: pulsation curve computed from the ephemeris; shaded region: the time *XMM* of the observation.
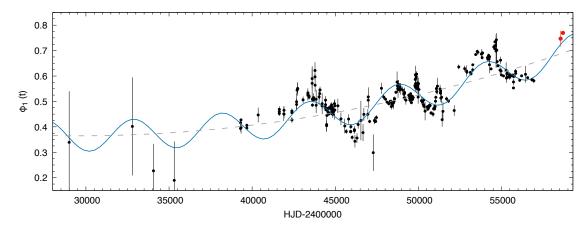

Figure 4. Long-term phase variation V473 Lyrae, based on the ϕ_1 Fourier term. The dashed line is a quadratic term describing a continuous decrease in period. The blue line shows the longer modulation cycle superimposed. This plot is an updated version of Fig. 9 by Molnar & Szabados (2014), and includes photometric data from Molnar et al. (2017), and Appendix A. The red dots on the far right are from Appendix A and the TESS data.

Figure 5. *TESS* observations of V473 Lyr.

3. RESULTS

The new observation of V473 Lyr is shown in Fig. 6 in the context of other Cepheid X-ray observations. δ Cep observations from Engle et al. (2017) are for both quiescent and burst states. β Dor observations include those from Engle (2015) supplemented by additional observations. For β Dor, the earlier phase (phase 0.25 on the left in Fig. 6) is computed from the ephemeris using light maximum. However, β Dor is in the period range near 10 days (P = 9.84^d) where a resonance decreases the pulsation amplitude and causes a distortion at maximum light. Since there are *HST* COS (Cosmic Origins Spectrograph) spectra (Engle 2015) the phase of minimum radius is well defined by ultraviolet emission lines caused by the passage of the pulsation wave through the photosphere and chromosphere. We can use this as the pulsation fiducial for the relation of minimum radius to the X-ray increase. Using this fiducial, the phase of the X-ray increase for β Dor is shifted to the righthand x symbol in Fig 6. Upper limits for random phase Cepheid observations are from Evans et al. (2016a). Fig. 6 shows that the X-ray observations for two cycles of δ Cep and also β Dor in the phase range 0.4 to 0.5 near maximum radius are well above the quiescent range for other phases of δ Cep.
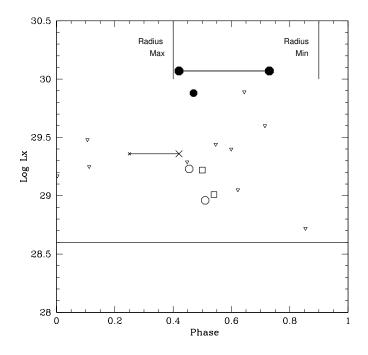
Figure 6. Cepheid X-ray observations as a function of pulsation phase. Filled circles: observations of V473 Lyr, with the phase range of the recent observation indicated by the joined circles; open circles and squares: δ Cep, with different symbols indicating different cycles; x's: β Dor: the phase on the right is adjusted to the phase based on photospheric emission lines (see text); open triangles: upper limits for other Cepheids; solid line at log $L_X = 28.6$: δ Cep in quiescent phases. The 2 vertical lines at the top indicate maximum and minimum radius of δ Cep. Luminosity is in ergs s^{-1}.

Both observations of V473 Lyr are well above even this bright X-ray luminosity. Furthermore they cover the phase range which extends over a third of the pulsation cycle, in contrast to the restricted phase range of δ Cep and β Dor. Although the cause of the X-ray bursts in δ Cep and β Dor is not yet understood, the X-ray luminosity of V473 Lyr does not appear to share the same characteristics of a much lower quiescent flux for most phases, but a short X-ray burst at the phase of maximum radius.

4. DISCUSSION

The X-ray source detected for V473 Lyr is relatively constant with phase, unlike those seen for δ Cep and β Dor, making it much more likely that the X-rays are produced by a young low mass companion than pulsation. The source is soft (kT = 0.6 keV), which would be consistent with a G or K main sequence companion at the age of the Cepheid (younger than the Pleiades; Preibisch and Feigelson 2005). A cool companion is consistent with the upper limit to a companion spectral type of A6 from an *IUE (International Ultraviolet Explorer)* spectrum (Evans 1992). We note that while G or K stars are common in the field population, *young* G and K stars are very rare, except in places such as open clusters.

A companion is surprising as there was no previous evidence that the Cepheid is a member of a spectroscopic binary. Identifying binary properties in a V473 Lyr system is, of course, complicated by variations due to pulsation, including the variable amplitude. MS discuss possible orbital velocity variation based on the velocities of Burki (2006) in connection with a third (5290^d) modulation in V473 Lyr. Fig. 7 shows the radial velocities over nearly 40 years. Velocities before JD 2452000 are CORAVEL velocities as discussed by Burki (2006, kindly made available by the Geneva Observatory), listed in Appendix C. More recent velocities are from Molnar, et al. (2017) and Appendix B. The bottom panel in Fig. 7 shows the residuals after correction for pulsation including modulation, based on the analysis of MS.

Residuals in the lower panel in Fig 7 sometimes exceed the typical CORAVEL error of 1 km s^{-1} (e.g. Evans, et al. 2015), although the scatter in measures obtained on the same night (Appendix C) suggest 1 km s^{-1} is a reasonable estimate. In order to look for multi-year velocity variations which might come from orbital motion, we have explored the data in two ways. First, we have binned data into one year segments to look at the mean and standard deviation. (Since the velocity uncertainties in the Appendix are all very similar, we have used no weighting.) Fig. 8 shows the mean and standard deviation in these bins. The means are typically within ±0.2 km s^{-1}, which is consistent with the
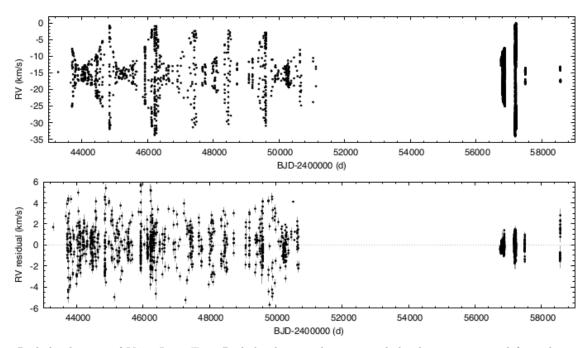
Figure 7. Radial velocities of V473 Lyr. Top: Radial velocities; bottom: radial velocities corrected for pulsation including modulation (see text)
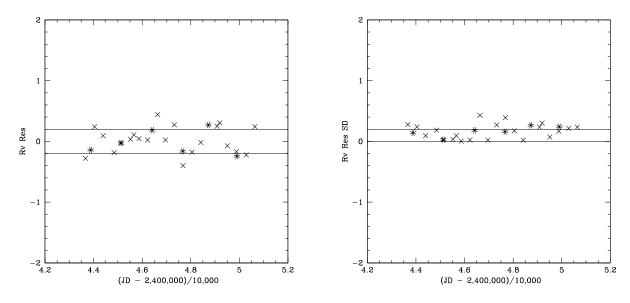

Figure 8. Left: Radial velocities binned into a year (x) and in periods of low amplitude (*). Each bin is plotted using the first JD of the bin. Lines indicate ± 0.2 km s^{-1}. Right: Standard deviation of each bin. Symbols are the same as left plot.

standard deviations within each bin.

The second approach is as follows. Since the amplitude of the pulsation is very small for some periods, corrections for pulsation should also be very small. We have identified periods of low amplitude and created the means and standard deviations in those bins. As shown in Fig. 8 by asterisks, the means and sd at these modulation phases are very similar to the results for the annual means. This demonstrates that the corrections for pulsation are accurate (for both high and low amplitude phases) and confirms the values for the annual means. In summary Fig. 8 provides an estimate of velocity variations of 0.2 km s^{-1} due to orbital motion over the 17 year coverage.

Comparison of proper motions from *Hipparcos* and *Gaia* (DR2) can reveal orbital motion (proper motion anomalies or PMa), as fully discussed by Kervella, et al. (2019). Fig. 9 shows the constraints on the combination of companion mass M$_2$ and radius (using a circular orbit) found from the *lack* of a significant PMa. The figure shows that an orbit of
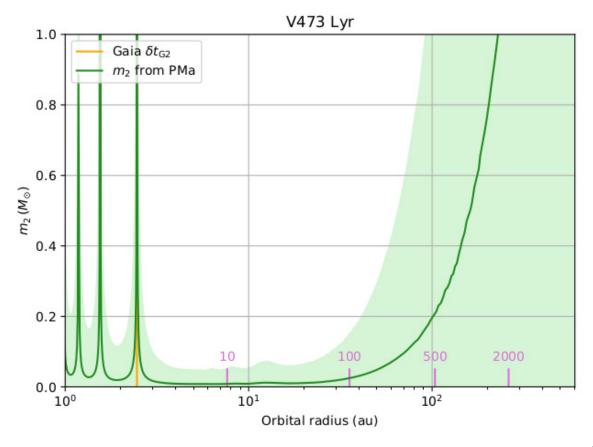
Figure 9. The constraints on the orbit from *Gaia* proper motions. X-axis: orbital radius in au and orbital periods (pink) in years; Y-axis: companion mass in $M_\odot$; the green curve is the relation from the PMa, with the light green shading indicating a one σ uncertainty; the yellow line is the orbital radius corresponding to *Gaia* DR2 time window of 688^d. (Plot created using the techniques described in Kervella, et al. 2019).
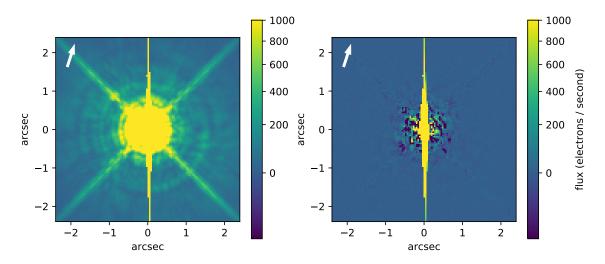

Figure 10. The HST WFC3 image of V473 Lyr. Left: Original image. Right: Point spread corrected image. The arrow points North.

3 au or one of more than 30 au would be compatible with a companion mass of at least a several tenths of a solar mass, but between them a stellar mass companion is unlikely. Furthermore, below 3 au there are only the very restricted peaks related to aliases of the time window of the *Gaia* DR2 data. It is unlikely that an orbital period would happen to fall in these limited regions.

Based on the proper motion constraint on orbits, we can estimate possible orbital velocities for the V473 Lyr system.

For the Cepheid we use a mass of 4 $M_\odot$, based on the mass of V1334 Cyg (Gallenne, et al. 2018). The X-ray luminosity of the companion is consistent with a G star at the age of the Cepheid (Preibisch and Feigelson 2005). There is some scatter in the age–spectral type–luminosity relations, but 1 $M_\odot$ is a reasonable estimate for the companion. A semi-major axis of 3 au corresponds to an orbital period of 2.3 years with these values. Note that orbits with Cepheid primaries all have periods of a year or more (Evans, et al. 2015) since shorter period systems would have undergone Roche lobe overflow when the primary became a red giant. For Cepheid masses, an orbit with a period of a year corresponds to an orbital radius of 1.7 au. A simple circular orbit with a period of 2.3 years would have a Cepheid velocity of 10 km s^{-1} and companion velocity of 39 km s^{-1}. These numbers will be reduced, of course, if the orbit is inclined or eccentric. Comparable velocities for a 30 au orbit (0.05") with a 73 year period become 2.7 km s^{-1} for the Cepheid and 11 km s^{-1} for the companion. The velocity data (Fig. 7 and Fig. 8) make the short period orbit very unlikely, requiring a very small inclination. This is particularly true since a period of nearly 20 years is very well covered by the Burki data. An orbit of 30 years or longer remains possible.

There is also a constraint on the outer size of the orbit. Seventy Cepheids have been surveyed with the HST Wide Field Camera 3 (WFC3) to detect resolved companions (Evans, et al. 2016b). The final analysis uses point spread corrected images as described in Evans, et al. 2020). On the corrected images, companions as close as 0.5″ can be identified (Fig. 10). No such companions are detected to this limit for V473 Lyr. Using the distance 553 pc (Evans et al. 2016b, based on the Benedict, et al. 2007 Leavitt law calibration), this limits the companion to within 280 au. The parallax from *Gaia* provides a closer distance of 453 pc (hence a tighter limit). Furthermore, the *Gaia* data identified no wide common proper motion companions.

This identification of a low mass companion has two implications. First, low mass companions of Cepheids are difficult to identify, since the spectral energy distribution is similar to that of the Cepheid, and the companion is much fainter than the Cepheid. Thus the X-ray identification of such a companion is important in determining the distribution of mass ratios down to small values. Second, as discussed above, we have usually used X-ray observations to confirm that a resolved companion is young enough to be a Cepheid companion. In this case, the argument is reversed. The X-ray active companion is another confirmation that V473 Lyr is a young Pop I star itself, despite its unusual pulsation characteristics.

5. SUMMARY

We have observed V473 Lyr twice with *XMM* with the following results.

• The X-ray flux is reasonably constant through a large part of the pulsation cycle, implying that a low mass companion is the likely source.

• Limits on the orbit of the companion from *HST* images, *Gaia* proper motions, and radial velocities are consistent with a separation between 30 and 300 au.

• This is important both because such a companion is otherwise difficult to detect.

• Furthermore it confirms that V473 Lyr is a Pop I Cepheid, though an unusual one.

• The X-ray upper limits in Fig 6 indicate nine other Cepheids where a companion as bright as that for V473 Lye would have been detected.

REFERENCES

Benedict, G. F., MacArthur, B. E., Feast, M. F., et al. 2007, AJ, 133, 1810

Burki, G. 2006, JAAVSO, 35, 19

Cash, W. 1979, ApJ, 228, 939

Engle, S. G. 2015, PhD Thesis, James Cook Univ., arXiv 1504.02713

Engle, S. G., Guinan, E. F., Harper, G. M., et al. 2017, ApJ, 838, 67

Evans, N. R. 1992, ApJ, 284, 220

Evans, N. R., Berdnikov, L., Lauer, J. et al. 2015, AJ, 150, 13

Evans, N. R., Pillitteri, I., Wolk, S., et al. 2016a, AJ, 151, 108

Evans, N. R., Bond, H. E., Schaefer, G. H., et al. 2016b, AJ, 151, 129

Evans, N. R., Engle, S., Guinan, E., Neilson, H., Marengo, M., Matthews, L., and Guenther, H. M. 2018, PTA Proc, 6, 253

Evans, N. R. et al. 2020 in prep (Paper III)

Gaia Collaboration, Brown, A. G. A, Vallenari, A. et al. 2018, A&A, 616, A1

Gallenne, A., Kervella, P., Evans, N. R., et al. 2018, ApJ, 876, 121

Kaastra, J. S. 2017, A&A, 605, A51

Kervella, P., Arenou, F., Mignard, F., and Thévenin, F. 2019, A&A, 623, A72

Molnar, L. and Szabados, L. 2014, MNRAS, 442, 3222 (MS)

Molnar, L., Derekas, A., Szabo, R., et al. 2017, MNRAS, 466, 4009

Pillitteri, I., Evans, N. R., Wolk, S. J., and Syal, M. B. 2013, AJ, 145, 143

Preibisch, T. and Feigelson, E. D. 2005, ApJS, 160, 390

Ricker, G. R., Winn, J. N., Vanderspek, N., et al., 2014, SPIE, 9143, 20

Szabo, R., Kollath, Z., Molnar, L., et al. 2010, MNRAS, 409, 1244

6. APPENDIX A: PHOTOMETRY

Table 2 lists the photometry from 2019 Only the first few lines are provided here to show the scope of the data; the full dataset is included in the electronic version.

Table 2. Photometry of V473 Lyr

JD -2,400,000	V mag	sd mag
58553.5642	6.209	0.001
58553.5644	6.211	0.001
58553.5646	6.166	0.001
58553.5647	6.208	0.001
58553.5649	6.192	0.001
58553.5651	6.159	0.001
58553.5652	6.192	0.001
58553.5654	6.170	0.001
58553.5656	6.172	0.001

7. APPENDIX B: VELOCITIES (2019)

Table 3 lists the radial velocities from 2019 Only the first few lines are provided here to show the scope of the data; the full dataset is included in the electronic version.

Table 3. Radial Velocities of V473 Lyr in 2019

JD -2,400,000	V_R km s^{-1}	sd km s^{-1}
58559.580	-14.386	0.605
58559.587	-14.157	0.846
58559.595	-13.974	0.553
58559.602	-14.046	0.553
58559.610	-13.850	0.641
58559.617	-13.939	0.562

8. APPENDIX C: CORAVEL VELOCITIES

Table 4 lists the CORAVEL velocities discussed by Burki (2006). Only the first few lines are provided here to show the scope of the data; the full dataset is included in the electronic version.

Table 4. CORAVEL Velocities of V473 Lyr

JD -2,400,000	V_R km s^{-1}	sd km s^{-1}
43286.527	-14.81	0.39
43666.609	-17.99	0.49
43706.471	-25.24	0.37
43708.471	-13.04	0.38
43709.449	-25.05	0.39
43709.522	-24.93	0.44
43710.472	-7.89	0.38
43711.474	-12.56	0.37
43712.452	-24.87	0.38